Contents lists available at ScienceDirect

Journal of Pharmaceutical Analysis

journal homepage: www.elsevier.com/locate/jpa

Original article

Absolute bioavailability, dose proportionality, and tissue distribution of rotundic acid in rats based on validated LC-QqQ-MS/MS method

Haihua Shang [a, b], Xiaohan Dai [b], Mi Li [b], Yueyi Kai [b], Zerong Liu [b], Min Wang [b], Quansheng Li [b], Yuan Gu [b, c], Changxiao Liu [a, b, *], Duanyun Si [b, c, **]

[a] School of Pharmacy, Shenyang Pharmaceutical University, Shenyang, 110016, China
[b] State Key Laboratory of Drug Delivery and Pharmacokinetics, Tianjin Institute of Pharmaceutical Research, Tianjin, 300301, China
[c] Research Unit for Drug Metabolism, Chinese Academy of Medical Sciences, Tianjin, 300301, China

ABSTRACT

Rotundic acid (RA), an ursane-type pentacyclic triterpene acid isolated from the dried barks of *Ilex rotunda* Thunb. (Aquifoliaceae), possesses diverse bioactivities. To further study its pharmacokinetics, a simple and sensitive liquid chromatography with triple quadrupole mass spectrometry (LC-QqQ-MS/MS) method was developed and validated to quantify RA concentration in rat plasma and tissue using etofesalamide as an internal standard (IS). Plasma and tissue samples were subjected to one-step protein precipitation. Chromatographic separation was achieved on a ZORBAX Eclipse XDB-C$_{18}$ column (4.6 mm × 50 mm, 5 μm) under gradient conditions with eluents of methanol:acetonitrile (1:1, *V/V*) and 5 mM ammonium formate:methanol (9:1, *V/V*) at 0.5 mL/min. Multiple reaction monitoring transitions were performed at *m/z* 487.30 → 437.30 for RA and *m/z* 256.10 → 227.10 for IS in the negative mode. The developed LC-QqQ-MS/MS method exhibited good linearity (2−500 ng/mL) and was fully validated in accordance with U.S. Food and Drug Administration bioanalytical guidelines. Dose proportionality and bioavailability in rats were determined by comparing pharmacokinetic data after single oral (10, 20, and 40 mg/kg) and intravenous (10 mg/kg) administration of RA. Tissue distribution was studied following oral administration at 20 mg/kg. The results showed that the absolute bioavailability of RA after administration at different doses ranged from 16.1% to 19.4%. RA showed good dose proportionality over a dose range of 10−40 mg/kg. RA was rapidly absorbed in a dose-dependent manner and highly distributed in the liver. In conclusion, this study is the first to systematically elucidate the absorption and distribution characteristics of RA in rats, which can provide additional information for further development and evaluation of RA in drug metabolism and pharmacokinetic studies.

1. Introduction

Ilicis Rotundae Cortex (IRC), also known as "*Jiu Bi Ying*" in China, is the dried barks of *Ilex rotunda* Thunb. (Aquifoliaceae) and is a drinkable tea with medicinal values that has thousands of years of history of usage in oriental medicine. The plant is widely distributed throughout southern China. It has been extensively utilized for the prevention and treatment of fever, common cold, sore throats, rheumatic pains, abdominal pain, and diarrhea and is officially described in the Chinese Pharmacopoeia (2020 edition) [1]. The chemical constituents of IRC have been extensively studied, and its clinical application and development as a functional tea has attracted special consideration owing to its potential health benefits. There are ten Chinese patent medicine formulas containing IRC, retrieved from the Yaozhi Network Database-Chinese patent medicine prescription [2]. Among them, there are two Chinese herbal teas.

Rotundic acid (RA), a plant-derived and ursane-type pentacyclic triterpene acid, was identified as a major active ingredient of IRC and has been shown to exert extensive pharmacological effects, including antimicrobial [3,4], anti-inflammatory [5],

anticancer [6–13], and lipid-decreasing effects [14]. It has also been proven to alleviate type 2 diabetes and its complications by improving the composition of the gut microbiota [15]. In addition, RA can increase the efficacy and reduce the side effects of radiotherapy via the ataxia-telangiectasia mutated (ATM)/p53 pathway [16]. RA is also found in various plants other than IRC, including *Guettarda platypoda* [17], *Mussaenda macrophylla* [18], and *Olea europaea* [19]. Although numerous pharmacological studies have shown that RA has various biological activities in vivo and in vitro, the preclinical absorption and distribution characteristics of RA are still unclear, which limits its clinical application and development. To date, analytical studies have focused only on the quantitation of RA in plants and decoction pieces, whereas the transporters and disposition of RA have scarcely been reported. Therefore, evaluating the pharmacokinetic properties of RA is important.

As an ursane-type pentacyclic triterpene, RA is also a highly hydrophobic compound with weak terminal ultraviolet absorption. Therefore, a high-performance liquid chromatography with ultraviolet (HPLC-UV) detection method is not suitable for analyzing the pharmacokinetics of RA. Currently, several methods have been reported for the determination of RA in plants, namely, HPLC-UV, HPLC with evaporation light scattering detector, and ultra-performance liquid chromatography with electrospray ionization quadrupole time-of-flight tandem mass spectrometry (UPLC/Q-TOF-MS/MS) [20–22]. However, no suitable method has been reported for the pharmacokinetic analysis of RA in biological samples. Liquid chromatography-MS/MS (LC-MS/MS) has become a crucial technique for the pharmacokinetic studies of natural products, and it is widely used for quantitative and qualitative analyses of active ingredients and metabolites in medicinal materials and Chinese patent medicines [23–27]. Hence, a novel LC-QqQ-MS/MS method for pharmacokinetic studies of RA in rats has been established and fully validated according to the bioanalytical guidelines recommended by the U.S. Food and Drug Administration (FDA). This is the first study to systematically address the plasma pharmacokinetic characteristics and tissue distribution of RA in rats. In addition, the results of this investigation will provide a basis for further development and clinical application of RA.

2. Experimental

2.1. Chemicals and materials

RA (purity > 98.6%, Lot No. 18110902) was manufactured by Chengdu Pufei De Biotech Co., Ltd. (Chengdu, China). The internal standard (IS) etofesalamide (Lot No. 100680–200901) was purchased from National Institute for the Control of Pharmaceutical and Biological Products (Beijing, China). Methanol and acetonitrile for HPLC were provided by Fisher Scientific (China) Co., Ltd. (Shanghai, China). Analytical-grade ammonium formate (AF) was obtained from Tianjin Guangfu Fine Chemical Research Institute (Tianjin, China). Highly pure deionized water was manufactured by a BM-40 water purification system from Zhongsheng Maoyuan Tech. Co., Ltd. (Beijing, China). All other used reagents were of analytical grade. Male Sprague–Dawley rats were obtained from SiPeiFu Biotechnology Co., Ltd. (Beijing, China). Blank rat heparinized plasma and tissue homogenates were obtained from healthy rats and stored in a −20 °C freezer before analysis.

2.2. Instruments

Samples were analyzed on an LCMS-8060 system (Shimadzu, Tokyo, Japan) equipped with an electrospray ionization (ESI) source and consisted of a binary LC-30AD delivery pump, a DGU-20A$_{5R}$ on-line degasser, a CTO-20A column oven, a SIL-30AC autosampler, and a CBM-20A system controller. Data acquisition and quantitation were performed using the LabSolutions LCMS Version 6.83 software (Shimadzu, Tokyo, Japan).

2.3. LC-MS/MS analysis

Chromatographic separation of the analytes was performed on an Agilent ZORBAX Eclipse XDB-C$_{18}$ column (4.6 mm × 50 mm, 5 μm; Santa Clara, CA, USA) at 40 °C and a flow rate of 0.5 mL/min for 6.5 min. The gradient elution solvent used consisted of methanol:acetonitrile (1:1, *V/V*) (A) and 5 mM AF aqueous solution:methanol (9:1, *V/V*) (B). The gradient elution program was set as follows: 0–3.00 min, 40%–10% B; 3.00–5.00 min, 10% B; 5.00–5.10 min, 10%–40% B; and 5.10–6.50 min, 40% B. From 2.0 to 3.2 min, the elution was injected into the MS detector, and the remainder was diverted to waste. The injection volume was 2 μL. All processed samples were maintained in the autosampler at 6 °C.

Multiple reaction monitoring (MRM) in the negative mode was selected and used to detect and quantify analytes. The ESI source was used to monitor ions, including precursor ion and product ion, *m/z* 487.30 $[M-H]^- \rightarrow$ 437.30 for RA and *m/z* 256.10 $[M-H]^- \rightarrow$ 227.10 for IS. The optimal parameters for MS were as follows: nebulizing gas flow, 3 L/min; heating gas and drying gas flow, 10 L/min; desolvation line temperature, 250 °C; interface temperature, 300 °C; and heat block temperature, 400 °C. The optimized compound parameters, including collision energy (CE), dwell time, Q1 and Q3 voltages, and precursor and product ions, are shown in Table 1.

2.4. Preparation of calibration standards and quality control (QC) samples

Stock solutions of RA (1 mg/mL) and IS (1 mg/mL) were prepared in methanol. A series of standard working solutions (0.04, 0.08, 0.4, 1, 4, 8, and 10 μg/mL) were prepared using the stock solution of RA. The RA working solutions were diluted with methanol, whereas the IS working solution (1 ng/mL) was diluted with acetonitrile. All stock and working solutions were properly stored in a refrigerator (4 °C) and warmed to room temperature (RT) for 15 min before use.

To obtain calibration standards, 475 μL of blank rat plasma or tissue homogenates (prepared by 50% methanol, 1:5, *m/V*) in polythene tubes were spiked with an aliquot of 25 μL of standard working solutions. The concentrations of RA were constructed in the range of 2–500 ng/mL for plasma and 10–2500 ng/g for tissue homogenates. QC samples (5, 40, and 375 ng/mL for plasma; 25, 200, and 1875 ng/g for tissue homogenates) were prepared in the same manner. All calibration standards and QC samples for each analysis batch were prepared daily. The spiked plasma or tissue homogenate samples were processed according to the sample preparation procedures.

2.5. Sample preparation

For RA analysis, rat plasma and tissue homogenate samples were subjected to protein precipitation. Samples (0.2 g) of tissues were homogenized with 500 μL of methanol and 500 μL of water. The plasma samples or tissue homogenates (50 μL), methanol (50 μL), and IS working solution (1 ng/mL, 100 μL) were transferred individually into 1.5 mL polythene tubes. Subsequently, the tubes were vigorously vortex-mixed for 1 min. After centrifugation for 10 min at 12,000 r/min and 4 °C, the resulting supernatant was placed into an insert tube, which was then

Table 1
Mass spectrometry compound parameters for rotundic acid (RA) and etofesalamide (internal standard, IS).

Analytes	Precursor (m/z)	Product (m/z)	Dwell time (ms)	Q1 Pre bias (V)	Collision energy (V)	Q3 Pre bias (V)	Retention time (min)
RA	487.30	437.30	200	24	35	15	2.78
IS	256.10	227.10	200	27	18	14	2.46

centrifuged under the above mentioned conditions. An aliquot of 2 μL of the supernatant was injected into the LC-MS/MS system for analysis.

2.6. Method validation

This bioanalytical assay was validated in compliance with the principles of Bioanalytical Method Validation Guidance for Industry promulgated by the FDA [28] with specific aspects described below. A full and systematic validation study was carried out for the determination of RA in rat plasma. To conduct partial validation studies, the same treatment and analysis methods as those for rat plasma samples were used for rat tissue homogenate samples, including brain, liver, and heart tissues as the representative tissues.

2.6.1. System suitability

To prove the system suitability of the assay, we analyzed the chromatograms of the working standard solution of RA containing the IS at a concentration of 20 ng/mL (three replicates of the two samples). System suitability was validated by within-run and between-run experiments. The relative standard deviation (RSD) calculated from six continuous peak area ratios (RA/IS) should be below 6% [29].

2.6.2. Selectivity and specificity

To investigate the potential interference for RA and IS, blank samples (heparinized rat plasma or tissue homogenates) from six different sources, lower limit of quantification (LLOQ) samples, and unknown samples collected after oral administration of RA were analyzed. The responses of interfering components at the RA and IS retention time in the blanks should be below 20% of the average RA responses of LLOQ samples and 5% of the average IS responses of the calibrators and QC samples, respectively.

2.6.3. Sensitivity and linearity

To evaluate the sensitivity of the method, different LLOQ samples (2 ng/mL for plasma and 10 ng/g for tissue homogenates) were prepared and assayed in six replicates, the responses of which should not be five times less than that of the zero calibrator (blank plasma/tissue homogenates plus IS). The linearity of this method was evaluated using calibration curves in the range of 2–500 ng/mL for rat plasma and 10–2500 ng/g for tissue homogenates. Calibration curves were constructed by plotting the peak area ratios (RA to IS, y) against the standard solution concentration of RA (x). Using a least-square regression model, the equation of linear regression was expressed as $y = ax + b$ with a weighting factor of $1/x^2$, and the correlation coefficient (r) should be greater than 0.99. The back-calculated concentrations of standards from the nominal concentration were required to be within ±15% (±20% for LLOQ).

2.6.4. Carryover

To assess the carryover effect of RA in the present method, blank rat plasma samples or tissue homogenates were immediately injected in triplicate following six consecutive injections of upper limit of quantification (ULOQ) samples. The appearance of RA in the rat blank plasma or tissue homogenate samples should be less than 20% of that obtained from LLOQ samples and 5% for the IS.

2.6.5. Cross talk

Cross talk between RA and IS was evaluated after separate injection of the zero calibrator and a ULOQ sample containing only RA. The acceptable response of RA from the zero calibrator was required to be below 20% of the mean response in the LLOQ sample. The acceptable response of IS obtained from the ULOQ (containing only RA) sample should not exceed 5% of the mean response in the LLOQ sample.

2.6.6. Accuracy and precision

The within-run and between-run accuracy and precision of the method were evaluated by sets of QC samples in three independent runs conducted over 3 days for plasma samples and in one run for tissue homogenate samples. Four concentration levels of QC samples were prepared in six replicates, including LLOQ, low QC (LQC), medium QC (MQC), and high QC (HQC). The precision of this assay was expressed as the RSD, and the between-run precision was calculated by using one-way analysis of variance (ANOVA). The assay accuracy was determined as a percentage of the nominal concentrations. Within-run precision and accuracy were assessed through analysis of six replicates of each concentration with QC samples in a single validation run. Between-run accuracy and precision were determined by 18 replicates analysis of each concentration conducted over 3 days. The acceptable within-run and between-run accuracy should be within ±15% (±20% for LLOQ) of the nominal concentrations, and the precision (RSD) should be less than 15% (20% for LLOQ).

2.6.7. Matrix effect and extraction recovery

Matrix effect can affect the reproducibility and sensitivity of quantitative determination using LC-MS/MS, including increased baseline, shift in retention time, and ion suppression or enhancement. Matrix effect and extraction recovery were evaluated by three QC (LQC, MQC, and HQC) samples with IS (1 ng/mL), and each subject was analyzed in six replicates. Post-extraction spiked samples were prepared from six different sources of rat blank plasma or tissue homogenates. The matrix effect of this assay was estimated by comparing the analytes/IS peak area ratio in post-extraction spiked samples with those in the corresponding pure work solution and determined as IS-normalized matrix factor (ISMF). The matrix effect was acceptable if the RSD of the ISMF is less than 15%. The extraction recovery of the method was evaluated by calculating the peak response of pre-extraction spiked samples with those obtained from the post-extraction spiked samples at the equivalent amount. The acceptable extraction recovery should be within ±15% of the nominal concentrations with an RSD of less than 15%.

2.6.8. Dilution effects

To monitor the integrity of dilution, samples with a concentration beyond the ULOQ need to be diluted prior to sample

determination. Dilution QC (DQC) samples were prepared at a concentration of 7500 ng/mL for plasma and 18,750 ng/g for tissue homogenates, and then diluted 20 and 10 times with the corresponding blank matrix, respectively. The mean accuracy of the DQC samples should be within ±15% of the nominal concentration, and the precision (RSD) should not exceed 15%.

2.6.9. Stability

The goal of sample stability study was to examine all conditions that might be encountered by the samples during handling and storing. In this study, the stability of RA was assessed at LQC and HQC levels in three replicates, including bench-top stability at RT for 24 h, autosampler stability of the processed sample at 6 °C for 48 h, stability following three freeze−thaw cycles (−20 °C/RT), and long-term stability at −20 °C for 28 days. Accompanying calibration curves and QC samples were freshly prepared and determined in the same batch. The analyte stability was acceptable when the accuracy (% nominal) at each QC level was within ±15%.

2.7. Absolute bioavailability and dose proportionality study

The protocols of the pharmacokinetic study were approved by the Institutional Animal Care and Use Committee of Tianjin Institute of Pharmaceutical Research (Tianjin, China). All male Sprague−Dawley rats were kept in an animal house (humidity, 55% ± 15%; temperature, 23 ± 3 °C) for 1 week. Before pharmacokinetic study, the rats were fasted overnight with free access to water. Twenty-four male rats (280 ± 20 g) were randomly divided into four groups ($n = 6$). Groups 1−3 received RA orally at three dose levels (10, 20, and 40 mg/kg) suspended in 5% (m/V) aqueous suspension of gum arabic (2 mg/mL), and group 4 received a single intravenous (i.v.) dose (10 mg/kg) of RA via caudal vein (4 mL/kg). An amount of i.v. RA solution was prepared by dissolving an appropriate amount of RA in a mixed solvent containing N,N-dimethyl formamide (DMF), 0.1 M NaOH, and normal saline at a ratio of 25:10:65 ($V/V/V$). After administration of RA, 200 μL of blood samples were collected from the suborbital venous plexus at 0.0833, 0.25, 0.5, 1, 1.5, 2, 3, 4, 6, 8, 10, and 24 h. All blood samples were transferred into heparinized tubes and centrifuged for 5 min at 12,000 r/min and 4 °C. All sampled plasma supernatants were immediately stored in a −20 °C freezer until LC-MS/MS analysis.

2.8. Tissue distribution study

Twenty-four male rats (200 ± 20 g) were randomly divided into four groups ($n = 6$), and each group was orally administered a single 20 mg/kg dose of RA. At 0.0833, 0.25, 1, and 4 h, after isoflurane anesthesia, heparinized blood samples were collected via abdominal aorta, and tissues (brain, muscle, fat, testis, heart, liver, spleen, lung, kidney, stomach, and duodenal tissues) were isolated. The collected tissues were rinsed to remove blood with 0.9% NaCl and then blotted dry with filter paper. Approximately 200 mg of tissue was weighed accurately, homogenized in methanol:water (1:1, V/V), and frozen at −20 °C until assay.

2.9. Pharmacokinetic parameters and date analysis

Major pharmacokinetic parameters, such as area under the curve from 0 h to infinity (AUC$_{0-\infty}$), area under the curve from 0 to 24 h (AUC$_{0-24}$), elimination half-life ($t_{1/2}$), apparent volume of distribution (V_d), and clearance (CL), were calculated by utilizing the Phoenix WinNonlin 7.0 software (Certara, Princeton, NJ, USA)

via non-compartmental method. The peak plasma concentration (c_{max}) and time to reach c_{max} (t_{max}) were directly acquired from the specific experimental data of each subject. The oral absolute bioavailability (F %) of RA in rats was determined as (AUC$_{oral}$ $_{(0-24)}$ × Dose$_{i.v.}$)/(AUC$_{i.v. (0-24)}$ × Dose$_{oral}$) × 100%. All data collected in this study are shown as means ± standard deviation (SD). One-way ANOVA was used to compare dose-normalized AUC$_{0-24}$ and c_{max} across three oral dosage levels, and dose proportionality was assessed using the IBM SPSS Statistics 25.0 software (SPSS Inc; Chicago, IL, USA). Significant difference was assumed when $P < 0.05$.

The dose proportionality of RA was assessed over a dose range of 10−40 mg/kg using a power model ($Y = \alpha \times (dose)^{\beta}$) [30,31]. Linear regression of ln-transformed pharmacokinetic parameters Y (AUC$_{0-24}$ and c_{max}) by the ln-transformed dose was described in the form of $\ln(Y) = \ln(\alpha) + \beta \times \ln(dose)$, where β is the dose proportionality coefficient. Dose proportionality should be concluded if the 90% confidence interval (CI) for β was within the acceptance range $[1 + \ln(0.5)/\ln(r), 1 + \ln(2.0)/\ln(r)]$ [32], where r is the ratio of the highest to the lowest doses.

3. Results and discussion

3.1. Method development

3.1.1. Choice of internal standard

An appropriate IS is essential for MS quantitation to control the variability of extraction, HPLC injection, and ionization. For this study, pentacyclic triterpene acids (glycyrrhetinic acid, ursolic acid, oleanolic acid, etc.) were considered a good choice of IS. However, their physicochemical properties and chromatographic behaviors are quite different from those of RA. Finally, we found that etofesalamide was the most favorable IS in the present analysis because it has good stability and is not an endogenous substance in the plasma. In addition, its retention time was the closest to that of RA. Therefore, etofesalamide was selected as the IS. In previous studies [33−35], digoxin and tanshinone IIA were chosen as IS, respectively.

3.1.2. Optimization of mass spectrometry conditions

ESI source and the negative ion mode were selected for this method. To optimize the MS conditions, RA and IS were dissolved in methanol at a concentration of 100 ng/mL, and then the standard solutions were infused (at 5 μL/min) into a mass spectrometer. The analytes and IS in the full scan mode yielded predominantly [M−H]$^-$ as the precursor ions at m/z 487.3 for RA and m/z 256.1 for IS, respectively. The product ions of RA were abundant at m/z 437.3 and 469.3 at a CE of 30 V (Fig. 1A). After careful optimization of the MS conditions by using biological samples, the transition m/z 487.3 → 437.3, which gave a lower baseline and minor interference although the peak response of this transition was slightly lower than that of the transition m/z 487.3 → 469.3, was finally selected to quantify RA in biological samples. The abundant and stable precursor-to-product ion transition of IS was m/z 256.1 → 227.1 (Fig. 1B). The ion transition of RA selected in this assay was different from that previously reported [34,35], where the mass transition chosen for quantitation was m/z 487.34 → 469.33 for RA. The difference in the ion pair selected may be due to disparity in instruments. Other MS parameters have been optimized to obtain the best sensitivity to RA (Table 1).

3.1.3. Optimization of chromatographic conditions

To achieve rapid and selective separation, appropriate sensitivity, and elimination of matrix effect, we investigated multiple
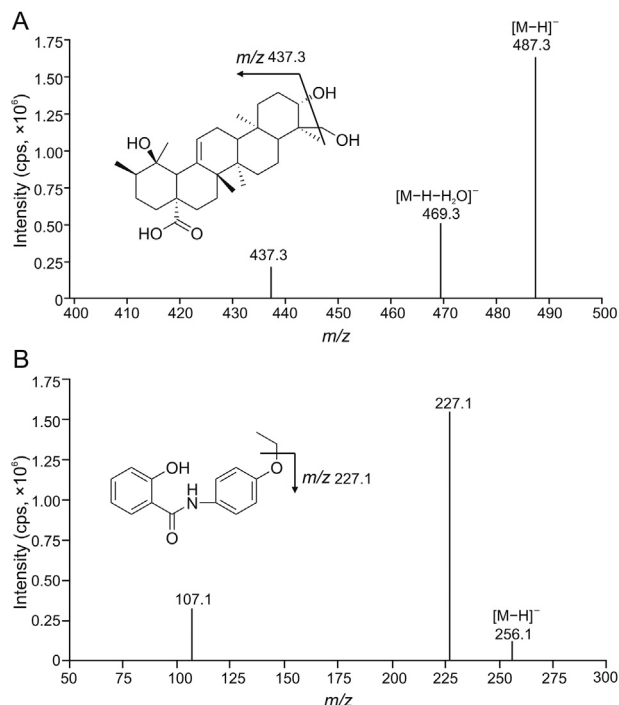
Fig. 1. Chemical structure and product ion mass spectra of (A) rotundic acid and (B) etofesalamide (internal standard).

chromatographic conditions, including the chromatographic column type, elution solvent compositions, and elution program selection. First, different chromatographic columns, such as Symmetry C_8 column (4.6 mm × 50 mm, 5 μm; Waters, Milford, MA, USA), ZORBAX Eclipse XDB-C_{18} column (4.6 mm × 50 mm, 5 μm; Agilent, Santa Clara, CA, USA), and ACQUITY UPLC BEH C_8 column (2.1 mm × 50 mm, 1.7 μm; Waters, Milford, MA, USA) were tested. Symmetry C_8 column has strong retention and long running time, whereas ACQUITY UPLC BEH C_8 column showed a poor peak shape and low sensitivity. Finally, ZORBAX Eclipse XDB-C_{18} column was selected for the chromatographic separation, as it displayed satisfactory performance with a good peak shape of analyte and IS, high sensitivity, and short running time.

Next, the different elution solvent compositions, including acetonitrile:water and methanol:water system, were optimized via a series of trials to achieve chromatographic separation of the sample. The results showed that methanol and acetonitrile at a ratio of 1:1 (*V/V*) were more suitable as an organic phase than pure methanol or acetonitrile solvent. The mixed organic phase had moderate retention time and low background noise, and the presence of AF in the aqueous phase was beneficial for the RA detection sensitivity and resulted in symmetrical peak shapes. Therefore, the final elution solvents comprised methanol:acetonitrile (1:1, *V/V*) as solvent A and 5 mM AF methanol (9:1, *V/V*) as solvent B. In the end, the isocratic and gradient elution procedures were compared to obtain the optimal chromatographic conditions with high sensitivity and selectivity. At approximately the same retention time of RA, we found that gradient elution resulted in better sensitivity and peak shape than isocratic elution. The optimal flow rate and injection volume were set to 0.5 mL/min and 2 μL, respectively.

3.1.4. Optimization of sample preparation conditions

Based on the analyte properties and matrix complexities, different biological sample processing techniques, including

protein precipitation (PPT), liquid–liquid extraction (LLE), and solid phase extraction (SPE), have been developed. It is generally known that LLE and SPE are not only time-consuming but also involve several tedious procedures. Therefore, a direct PPT process was selected for sample pretreatment in our study. To improve efficiency of extraction and decrease matrix effect, different precipitant solvents, including methanol, acetonitrile, and their mixed solution, were tested. Finally, the methanol and acetonitrile combination (1:2, *V/V*) was selected as extraction solvent in the current study owing to its high specificity and extraction effect. The sample processing procedure in this study was more convenient and better than previously reported UPLC/Q-TOF-MS/MS methods [34,35], which used methanol as the precipitant and involved centrifugation, vacuum drying, and reconstitution procedures. To ensure the stability of the samples in the homogenizing process, 50% methanol was used as medium for the preparation of tissue homogenate samples. The subsequent sample treatment process was the same as that for plasma samples.

3.2. Bioanalytical method validation

3.2.1. System suitability

System suitability test is an integral part of bioanalytical method, and it needs to be conducted before running samples, in every run, to ensure that the system is operating normally and the results are reliable. In this study, the RSD of six continuous peak area ratios (RA/IS) ranged from 4.37% to 4.74%, indicating that the performance of the LC-MS/MS system in this assay was good for the pharmacokinetic analysis of RA in biological samples.

#### 3.2.2. Selectivity and specificity

All blank plasma samples and tissue homogenates from six different origins were found to have no interfering peaks from endogenous and environmental constituents around the retention time of RA or IS, indicating that the method has good separation and excellent specificity. The typical chromatograms of rat blank plasma or liver homogenate, blank plasma or liver homogenate spiked with RA (LLOQ) and IS standard solution, and unknown plasma sample or liver homogenate are shown in Fig. 2. The retention time was 2.78 min for RA and 2.46 min for IS.

3.2.3. Linearity and sensitivity

The plasma or tissue homogenate calibration curve constructed using seven calibrators was found to be linear over different RA concentration levels: 2–500 ng/mL for plasma and 10–2500 ng/g for tissue homogenates. The regression equations of plasma or tissue homogenate are shown in Table 2. The accuracy of these standard sample concentrations back-calculated from the standard curve for rat plasma was within 97.6%–110% at all concentrations, whereas the precision ranged from 2.96% to 9.79%. Representative MRM chromatograms of RA and IS are presented in Fig. 2. The sensitivity (LLOQ), defined as the lowest

Table 2
Regression equation, correlation coefficient (*r*), and linear range of rotundic acid.

Matrix	Run (#)	Regression equation	*r*	Linear range
Plasma	1	$y = 0.00541x + 0.007631$	0.9981	2–500 ng/mL
	2	$y = 0.00552x + 0.001469$	0.9970	
	3	$y = 0.00508x + 0.001071$	0.9971	
Liver	1	$y = 0.00141x + 0.001125$	0.9984	10–2500 ng/g
Heart	1	$y = 0.00137x + 0.001093$	0.9959	
Brain	1	$y = 0.00127x + 0.0009889$	0.9976	
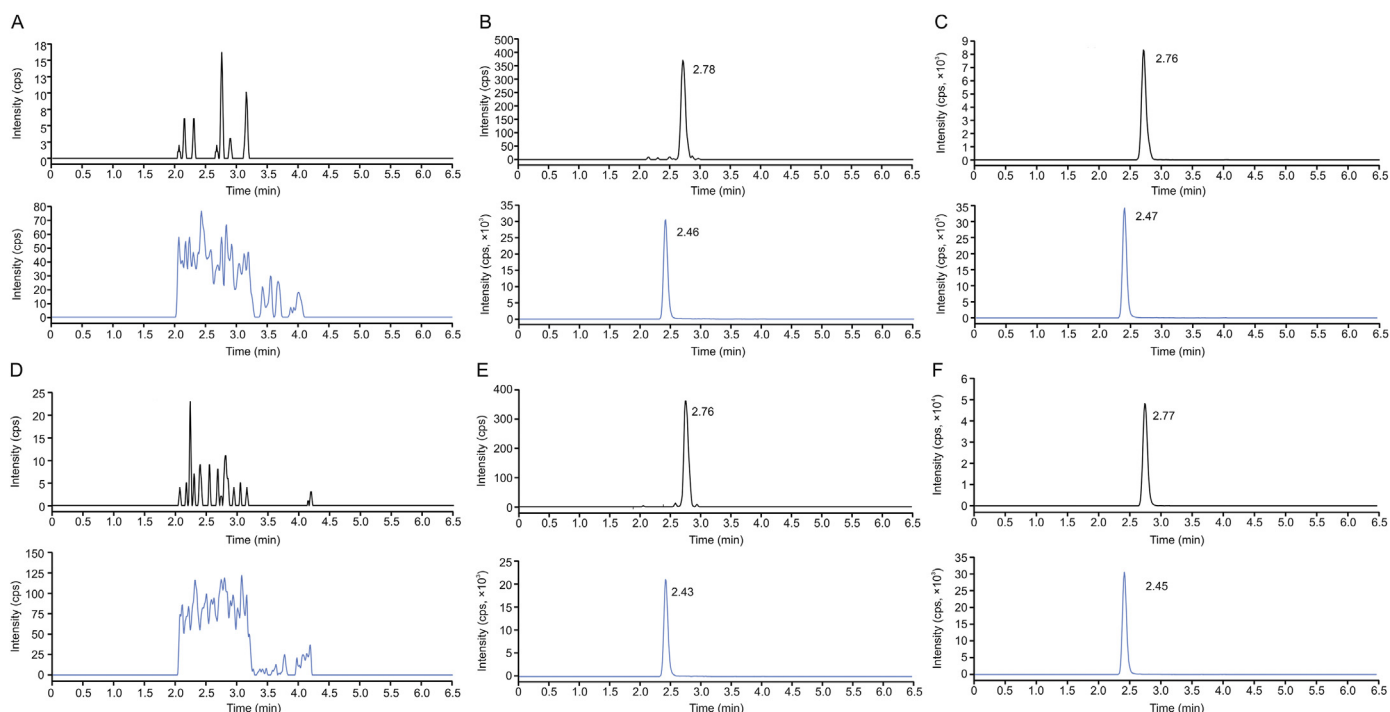
Fig. 2. Representative chromatograms of rotundic acid (RA) and etofesalamide (IS): (A) blank rat plasma sample and (D) liver homogenate; (B) blank plasma sample and (E) liver homogenate spiked with 2 ng/mL RA (lower limit of quantification) and 1 ng/mL IS; (C) plasma sample and (F) liver homogenate collected at 1 h after oral administration of 10 and 20 mg/kg RA, respectively.

Table 3
Within-run (*n*=6) and between-run (*n*=18) accuracy and precision of the developed method for the determination of rotundic acid.

Item	Matrix	Run (#)	LLOQ		LQC		MQC		HQC	
			Accuracy (%)	Precision (%)	Accuracy (%)	Precision (%)	Accuracy (%)	Precision (%)	Accuracy (%)	Precision (%)
Within-run	Liver	1	105	8.16	96.3	3.00	104	3.50	95.8	5.53
	Heart	1	106	5.27	104	6.64	103	5.65	94.6	3.41
	Brain	1	107	3.73	97.3	6.05	102	4.14	89.2	2.79
	Plasma	1	105	11.5	113	6.28	108	3.28	96.4	3.02
		2	111	9.69	112	6.08	105	1.88	92.8	1.95
		3	107	9.85	107	4.15	101	1.84	87.7	3.05
Between-run	Plasma	/	108	7.87	111	7.75	105	7.85	92.3	11.6

LLOQ: lower limit of quantification; LQC: low quality control; MQC: medium quality control; HQC: high quality control.

non-zero standard from the calibration curve, was found to be 2 ng/mL for plasma and 10 ng/g for tissue homogenates. The S/N ratio was more than 5 in LLOQ sample (Figs. 2B and E), and both the accuracy (% nominal) and precision (RSD) were within the acceptable ranges (Table 3). The LLOQ with 50 μL plasma (2 μL injection volume) achieved by the present method was lower than that achieved by previously reported UPLC/Q-TOF-MS/MS methods (3.2 and 2.88 ng/mL, respectively) with 100 μL plasma (5 μL injection volume) [34,35].

3.2.4. Carryover

After injecting six consecutive ULOQ samples, a blank control sample was injected immediately in triplicate. No signal was observed in the blank control sample at the corresponding retention times of both RA and IS, suggesting that the carryover of this standard analytical procedure was acceptable.

3.2.5. Cross talk

No RA signal was observed in the zero calibrator, and no IS signal was found in the ULOQ sample containing only RA, indicating that there was no cross talk between RA and IS.

3.2.6. Accuracy and precision

QC samples at four levels were used to evaluate the within-run and between-run precision and accuracy in six replicates. The

Table 4
Matrix effect and extraction recovery of rotundic acid (*n*=6).

Matrix	QC levels	Matrix effect (%)		Extraction recovery (%)	
		Mean	RSD	Mean	RSD
Plasma	LQC	95.6	6.28	100	3.23
	MQC	92.8	4.86	98.6	3.04
	HQC	82.6	0.94	101	5.44
Liver	LQC	89.9	3.23	102	5.90
	MQC	92.9	4.51	105	4.85
	HQC	88.6	4.07	92.4	2.90
Heart	LQC	97.3	6.01	97.9	2.47
	MQC	96.3	3.18	98.5	5.27
	HQC	87.3	3.70	105	3.12
Brain	LQC	97.7	5.69	101	3.77
	MQC	99.7	5.07	104	5.15
	HQC	93.2	4.08	98.1	5.26

QC: quality control; LQC: low quality control; MQC: medium quality control; HQC: high quality control; RSD: relative standard deviation.

Table 5
Stability of rotundic acid in different matrix under various storage conditions ($n=3$).

Stability	Conditions	Matrix	LQC		HQC	
			Accuracy (%)	Precision (%)	Accuracy (%)	Precision (%)
Bench-top	24 h at RT	Plasma	113	8.06	95.7	2.25
		Liver	101	3.54	98.4	4.07
Autosampler ($n=6$)	48 h at 6 °C	Plasma	101	4.31	97.0	3.64
		Liver	95.0	2.64	108	4.13
Three freeze-thaw cycles	−20 °C to RT	Plasma	110	3.92	99.3	3.55
		Liver	102	6.98	110	5.97
Long-term	28 days at −20 °C	Plasma	110	3.90	105	4.40
		Liver	104	3.72	95.4	4.93

RT: room temperature; LQC: low quality control; HQC: high quality control.
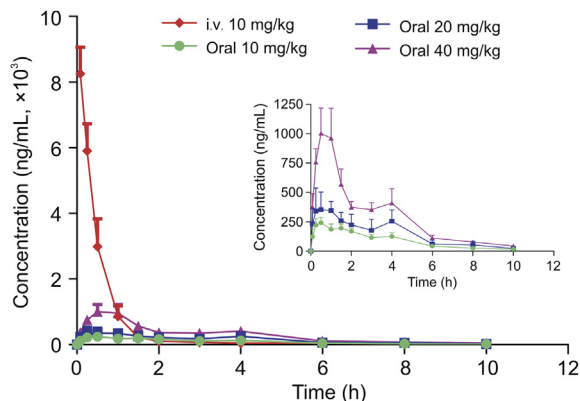
Fig. 3. Mean plasma concentration profile of rotundic acid versus time following intravenous (i.v.) administration to rats at 10 mg/kg and oral administration at 10, 20, and 40 mg/kg. The data are presented as mean ± standard deviation (SD) ($n=6$).

Table 6
Main parameters of the plasma pharmacokinetics of rotundic acid in rats after oral or intravenous (i.v.) administration (mean ± SD, $n=6$).

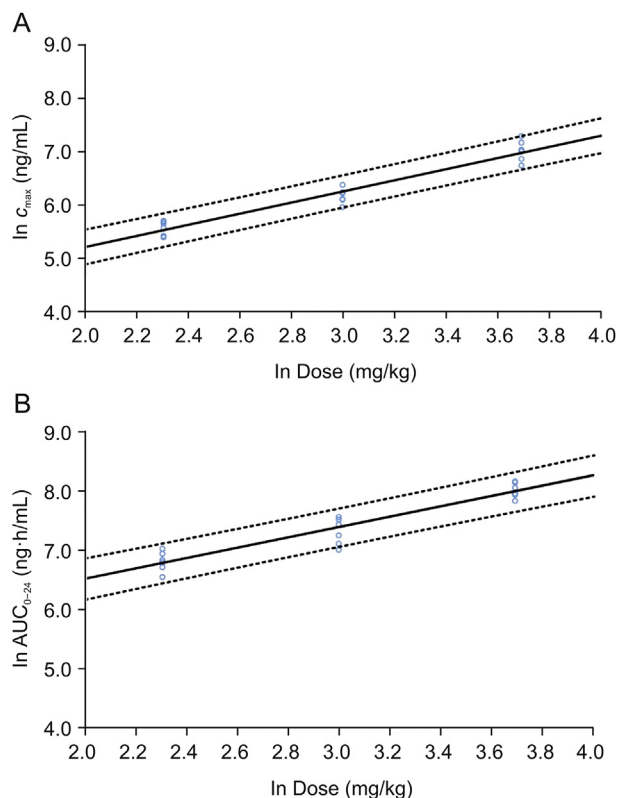| Parameters	Oral			i.v. 10 mg/kg
	10 mg/kg	20 mg/kg	40 mg/kg	
c_{max} (ng/mL)	263 ± 34.5	479 ± 68.6	1130 ± 225	8250 ± 814
t_{max} (h)	0.542 ± 0.485	0.542 ± 0.368	0.750 ± 0.274	/
AUC_{0-24} (ng·h/mL)	914 ± 151	1520 ± 331	3020 ± 384	4700 ± 760
$AUC_{0-\infty}$ (ng·h/mL)	969 ± 164	1600 ± 380	3240 ± 545	4770 ± 768
MRT_{0-24} (h)	2.82 ± 0.373	3.02 ± 0.553	2.73 ± 0.187	0.692 ± 0.106
$MRT_{0-\infty}$ (h)	3.34 ± 0.567	3.44 ± 0.780	3.55 ± 0.886	0.906 ± 0.157
V_d (L/kg)	30.8 ± 7.08	38.8 ± 6.99	52.5 ± 20.2	9.41 ± 3.53
CL (L/h/kg)	10.6 ± 1.92	13.2 ± 3.22	12.6 ± 2.08	2.15 ± 0.376
$t_{1/2}$ (h)	2.07 ± 0.571	2.08 ± 0.295	3.06 ± 1.71	3.02 ± 0.947
F (%)	19.4	16.2	16.1	/

SD: standard deviation; c_{max}: peak plasma concentration; t_{max}: time to reach c_{max}; AUC_{0-24}: area under the curve from 0 to 24 h; $AUC_{0-\infty}$: area under the curve from 0 h to infinity; MRT_{0-24}: mean residence time from 0 to 24 h; $MRT_{0-\infty}$: mean residence time from 0 h to infinity; V_d: apparent volume of distribution; CL: clearance; $t_{1/2}$: elimination half-life; F: bioavailability.

accuracy and precision of the present analytical method are reported in Table 3. For plasma samples, the within-run accuracy ranged from 87.7% to 113%, with the precision ranging from 1.84% to 11.5%. The between-run accuracy was from 92.3% to 111%, with the

Fig. 4. Dose proportionality of rotundic acid (c_{max} and AUC_{0-24}) following oral administration to rats at a dose range of 10–40 mg/kg. The empty circles represent the observed values, the solid lines are the regression lines based on the observed data, and the dashed lines are the 90% confidence interval. (A) c_{max}, (B) AUC_{0-24}. c_{max}: the peak plasma concentration; AUC_{0-24}: area under the curve from 0 to 24 h.

precision ranging from 7.75% to 11.6%. For tissue homogenates, the within-run accuracy ranged from 89.2% to 107%, with the within-run precision ranging from 2.79% to 8.16%. These results indicated that the current approach developed for quantifying RA in rat plasma and tissue homogenates was reliable, accurate, and reproducible.

Table 7
Assessment of dose proportionality of rotundic acid based on the power model.

Parameter	Linearity range (mg/kg)	R^2	β (Mean ± SE)	90% confidence interval (CI)	Acceptance range
c_{max}	10–40	0.933	1.044 ± 0.070	0.921–1.166	0.500–1.500
AUC_{0-24}	10–40	0.893	0.865 ± 0.075	0.735–0.996	0.500–1.500

c_{max}: the peak plasma concentration; AUC_{0-24}: area under the curve from 0 to 24 h; R^2: coefficient of determination; β: dose proportionality coefficient; SE: standard error.

Table 8
Tissue distribution of rotundic acid following oral administration to rats at 20 mg/kg (mean ± SD, n=6).

Sample	Concentrations of RA (ng/g)				AUC$_{0-4}$ (ng·h/g)	Tissue/Plasma ratio
	0.0833 h	0.25 h	1 h	4 h		
Plasma[a]	85.9 ± 25.8	992 ± 508	576 ± 233	55.1 ± 2.35	1627	1.00
Brain	0 ± 0	57.7 ± 22.5	0 ± 0	0 ± 0	26.4	0.0162
Heart	1728 ± 1116	763 ± 304	241 ± 82.0	0 ± 0	1017	0.625
Liver	653 ± 303	5889 ± 1451	2206 ± 1580	461 ± 123	7608	4.68
Spleen	948 ± 400	502 ± 215	160 ± 24.8	0 ± 0	649	0.399
Lung	6446 ± 2794	646 ± 241	170 ± 66.0	12.3 ± 21.4	1438	0.884
Kidney	2027 ± 868	1213 ± 206	456 ± 155	63.0 ± 19.1	1758	1.08
Stomach	6374 ± 1986	7126 ± 1915	2463 ± 625	43.3 ± 11.5	8746	5.38
duodenum	6174 ± 3998	4684 ± 1672	1915 ± 2222	0 ± 0	6508	4.00
Muscle	868 ± 284	348 ± 78.1	111 ± 17.3	0 ± 0	475	0.292
Fat	706 ± 335	713 ± 269	427 ± 422	0 ± 0	1215	0.747
Testis	143 ± 71.0	759 ± 321	124 ± 64.9	21.3 ± 18.5	629	0.387

[a] Concentration unit: ng/mL. SD: standard deviation; AUC$_{0-4}$: area under the curve from 0 to 4 h. Tissue/Plasma ratio: the tissue AUC$_{0-4}$/the plasma AUC$_{0-4}$.

3.2.7. Matrix effect and extraction recovery

The RSD of the ISMF and the mean extraction recoveries of RA from plasma or tissue homogenates at three QC levels (LQC, MQC, and HQC) were found to be well within the acceptable criteria (Table 4). It was suggested that the ion enhancement or suppression of the matrix in the method could be negligible, and the optimized RA extraction method was the simplest, most economical and efficient, and least time-consuming.

3.2.8. Dilution effect

The accuracy of DQC after dilution with blank plasma or tissue homogenates was in the range of 98.5%–102%, and the precision ranged from 1.99% to 5.89%, suggesting that this method can accurately determine RA concentration beyond the curve range.

3.2.9. Stability

RA stability was investigated at low and high concentrations under various possible expected conditions, including bench-top storage, long-term storage, autosampler storage, and freeze–thaw cycles. The RA stability data are enumerated in Table 5. Notably, RA was stable after being subjected to different storage and handling conditions, and the accuracy and precision of the predicted concentration were within the acceptable criteria. The accuracy values ranged from 95.0% to 113%, whereas the RSD values were less than 10%.

3.3. Absolute bioavailability and dose proportionality study

The plasma pharmacokinetics of RA following single i.v. administration (10 mg/kg) and oral administration at three doses (10, 20, and 40 mg/kg) in rats was successfully evaluated using the validated LC-QqQ-MS/MS method. The plots of mean plasma concentration (y-axis) versus time (x-axis) of RA are presented in Fig. 3. The corresponding pharmacokinetic parameters of RA are presented as mean ± SD in Table 6. After single i.v. administration in rats, the CL and V_d of RA were 2.15 ± 0.376 L/h/kg and 9.41 ± 3.53 L/kg, respectively (Table 6, Fig. 3). RA exhibited moderate clearance ($t_{1/2}$ = 3.02 ± 0.947 h), with 20%–70% hepatic blood flow (3.3 L/h/kg) [36,37] in rats. The mean V_d was approximately 14-fold greater than the total body water content in rats (0.67 L/kg) [36], suggesting the extensive tissue distribution of RA. After single oral administration, RA was found to be rapidly absorbed into the blood, with t_{max} observed within 0.75 h of dosing at three doses. RA showed poor oral exposure at 10, 20, and 40 mg/kg, with an absolute bioavailability (F%) of 19.4%, 16.2%, and 16.1%, respectively. The low oral bioavailability of RA could be due to its poor water-solubility, low intestinal permeability, hepatic first-pass metabolism, and high affinity to tissues.

The bioavailability in this study was different from that reported previously (4.52%) [33]. This may be owing to the difference in drug crystals and the preparation method of RA suspensions for oral administration to rats.

The dose proportionality of RA after single oral administration at three doses (10, 20, and 40 mg/kg) indicated that both the c_{max} and AUC$_{0-24}$ of RA increased with an increase in dose. The linear regression equation of $\ln(c_{max})$ and $\ln(AUC_{0-24})$ versus $\ln(dose)$ is $\ln(c_{max}) = 3.12 + 1.04 \ln(dose)$ and $\ln(AUC_{0-24}) = 4.78 + 0.87 \times \ln(dose)$, respectively. One-way ANOVA revealed no significant difference in CL, $t_{1/2}$, and dose-normalized pharmacokinetic parameters, including AUC$_{0-24}$ and c_{max}, among the three doses ($P>0.05$). The results of dose proportionality assessment based on the power model are presented in Table 7. The profiles of $\ln(c_{max})$ and $\ln(AUC_{0-24})$ versus $\ln(dose)$ after single oral administration of RA (10, 20, and 40 mg/kg) to rats with the associated 90% CI are presented in Fig. 4. The β (90% CI) was 1.044 (0.921–1.166) for c_{max} and 0.865 (0.735–0.996) for AUC$_{0-24}$, which were both within the acceptance interval (0.500–1.500), suggesting that RA showed good dose proportionality in the range of 10–40 mg/kg.

3.4. Tissue distribution study

The results of the tissue distribution study of RA in rats are displayed in Table 8. After a single oral (20 mg/kg) administration, RA was distributed rapidly (requiring 5–15 min to reach the peak) and extensively (detected in all tissues tested). Except in the stomach and duodenum, RA was distributed in all tissues tested, showing a tissue/plasma concentration ratio of 4.68 for liver tissue, 1.08 for kidney tissue, and less than 1.0 for other tissues, indicating that RA had high affinity for liver tissue, probably owing to its high lipophilicity. This may be the mechanism underlying its therapeutic effect on liver disease and may explain the large V_d estimated from the venous plasma concentration data. The content of RA in all tissues at 4 h after oral administration had decreased to less than 1/10 of the peak in the tissues, showing that no obvious accumulation of RA was found in tissues and that extensive metabolism or elimination of RA might have occurred in the liver. This could also be an important cause of its low oral bioavailability. Although the level of RA in the brain was the lowest, it was detected only at 0.25 h, which may suggest that RA did not easily cross the blood-brain barrier.

4. Conclusion

In the present study, a sensitive, specific, and simple LC-QqQ-MS/MS method was successfully established to quantify RA in

both rat plasma and tissues. In addition, the developed method in this study was fully validated for the first time in accordance with FDA guidelines for bioanalysis, and it was successfully applied to absolute bioavailability, dose proportionality, and tissue distribution studies of RA in rats. RA had a low absolute oral bioavailability (<20%) and was rapidly and extensively distributed following oral administration in rats. RA also exhibited a high concentration in the liver. The dose proportionality of RA revealed a good linear pharmacokinetic profile ranging from 10 to 40 mg/kg. These findings provide a theoretical basis for further research and development of RA either in vivo or in vitro.

CRediT author statement

Haihua Shang: Methodology, Formal analysis, Writing - Original draft preparation, Visualization, Investigation; **Xiaohan Dai:** Validation, Investigation, Resources; **Mi Li:** Validation, Formal analysis, Visualization; **Yueyi Kai:** Investigation, Resources; **Zerong Liu:** Investigation, Resources; **Min Wang:** Validation, Formal analysis; **Quansheng Li:** Data curation, Resources; **Yuan Gu:** Project administration, Conceptualization; **Changxiao Liu:** Writing - Reviewing and Editing, Conceptualization; **Duanyun Si:** Writing - Reviewing and Editing, Supervision.

Declaration of competing interest

The authors declare that there are no conflicts of interest.

Acknowledgments

References

[1] Chinese Pharmacopoeia Commission, Pharmacopoeia of the People's Republic of China, China Medical Science Press, Beijing, 2020, pp. 325.

[2] Yaozhi Network Database of Chinese Patent Medicine Prescription, China. https://db.yaozh.com/chufang/. (Accessed 20 October 2020).

[3] A.O. Aro, J.P. Dzoyem, M.D. Awouafack, et al., Fractions and isolated compounds from *Oxyanthus speciosus* subsp. *stenocarpus* (Rubiaceae) have promising antimycobacterial and intracellular activity, BMC Complement Altern. Med. 19 (2019), 108.

[4] H.T. Nguyen, D.V. Ho, H.Q. Vo, et al., Antibacterial activities of chemical constituents from the aerial parts of *Hedyotis pilulifera*, Pharm. Biol. 55 (2017) 787–791.

[5] T.D. Thang, P.-C. Kuo, C.-S. Yu, et al., Chemical constituents of the leaves of *Glochidion obliquum* and their bioactivity, Arch Pharm. Res. 34 (2011) 383–389.

[6] X.-F. Cao, J.-S. Wang, P.-R. Wang, et al., Triterpenes from the stem bark of *Mitragyna diversifolia* and their cytotoxic activity, Chin. J. Nat. Med. 12 (2014) 628–631.

[7] Y. Chen, Y.-F. He, M.-L. Nan, et al., Novel rotundic acid derivatives: synthesis, structural characterization and in vitro antitumor activity, Int. J. Mol. Med. 31 (2013) 353–360.

[8] Y.F. He, M.L. Nan, J.M. Sun, et al., Design, synthesis and cytotoxicity of cell death mechanism of rotundic acid derivatives, Bioorg. Med. Chem. Lett. 23 (2013) 2543–2547.

[9] Y.-F. He, M.-L. Nan, J.-M. Sun, et al., Synthesis, characterization and cytotoxicity of new rotundic acid derivatives, Molecules 17 (2012) 1278–1291.

[10] Y.-F. He, M.-L. Nan, Y.-W. Zhao, et al., Design, synthesis and evaluation of antitumor activity of new rotundic acid acylhydrazone derivatives, Z. Naturforsch. C J. Biosci. 71 (2016) 95–103.

[11] W.-J. Liu, Y.-Y. Peng, H. Chen, et al., Triterpenoid saponins with potential cytotoxic activities from the root bark of *Ilex rotunda* Thunb, Chem. Biodivers. 14 (2017), e1600209.

[12] M.-L. Nan, X. Wang, H.-J. Li, et al., Rotundic acid induces Cas3-MCF-7 cell apoptosis through the p53 pathway, Oncol. Lett. 17 (2019) 630–637.

[13] G. Roy, S. Guan, H. Liu, et al., Rotundic acid induces DNA damage and cell death in hepatocellular carcinoma through AKT/mTOR and MAPK pathways, Front. Oncol. 9 (2019), 545.

[14] Y.-M. Hsu, Y.-C. Hung, L. Hu, et al., Anti-diabetic effects of madecassic acid and rotundic acid, Nutrients 7 (2015) 10065–10075.

[15] Z. Yan, H. Wu, H. Yao, et al., Rotundic acid protects against metabolic disturbance and improves gut microbiota in type 2 diabetes rats, Nutrients 12 (2019), 67.

[16] Z.-F. Wang, W.-Y. Sun, D.-H. Yu, et al., Rotundic acid enhances the impact of radiological toxicity on MCF-7 cells through the ATM/p53 pathway, Int. J. Oncol. 53 (2018) 2269–2277.

[17] J. Bhattacharyya, M.Z. De Almeida, Isolation of the constituents of the root-bark of *guettarda platypoda*, J. Nat. Prod. 48 (1985) 148–149.

[18] N.C. Kim, A.E. Desjardins, C.D. Wu, et al., Activity of triterpenoid glycosides from the root bark of *Mussaenda macrophylla* against two oral pathogens, J. Nat. Prod. 62 (1999) 1379–1384.

[19] Y. Orihara, Y. Ebizuka, Production of triterpene acids by cell-suspension cultures of *olea europaea*, V.R. Preedy, R.R. Watson, Olives and Olive Oil in Health and Disease Prevention, Academic Press, New York, 2010, pp. 341–347.

[20] J.-B. Xie, Z.-M. Bi, P. Li, HPLC-ELSD determination of triterpenoids and triterpenoid saponins in *Ilex pupurea* leaves, Acta Pharm. Sin. 38 (2003) 534–536.

[21] B. Yang, H. Li, Q.-F. Ruan, et al., A facile and selective approach to the qualitative and quantitative analysis of triterpenoids and phenylpropanoids by UPLC/Q-TOF-MS/MS for the quality control of *Ilex rotunda*, J. Pharm. Biomed. Anal. 157 (2018) 44–58.

[22] J.P. Zhu, B. Yang, T. Yang, et al., Simultaneous determination of four constituents in Cortex ilicis Rotundae with HPLC, Tradit. Chin. Drug Res. Pharmaco. 26 (2015) 558–560.

[23] Y. He, Z. Wei, Y. Xie, et al., Potential synergic mechanism of Wutou-Gancao herb-pair by inhibiting efflux transporter P-glycoprotein, J. Pharm. Anal. 10 (2020) 178–186.

[24] D. Kang, Q. Ding, Y. Xu, et al., Comparative analysis of constitutes and metabolites for traditional Chinese medicine using IDA and SWATH data acquisition modes on LC-Q-TOF MS, J. Pharm. Anal. 10 (2020) 588–596.

[25] Y.-N. Tang, Y.-X. Pang, X.-C. He, et al., UPLC-QTOF-MS identification of metabolites in rat biosamples after oral administration of Dioscorea saponins: a comparative study, J. Ethnopharmacol. 165 (2015) 127–140.

[26] T. Yi, L. Zhu, Y.-N. Tang, et al., An integrated strategy based on UPLC–DAD–QTOF-MS for metabolism and pharmacokinetic studies of herbal medicines: Tibetan "Snow Lotus" herb (*Saussurea laniceps*), a case study, J. Ethnopharmacol. 153 (2014) 701–713.

[27] M. Liao, H. Shang, Y. Li, et al., An integrated approach to uncover quality marker underlying the effects of Alisma orientale on lipid metabolism, using chemical analysis and network pharmacology, Phytomedicine 45 (2018) 93–104.

[28] U.S. Food and Drug Administration, Bioanalytical method validation guidance for industry. https://www.fda.gov/regulatory-information/search-fda-guidance-documents/bioanalytical-method-validation-guidance-industry. (Accessed 24 May 2018).

[29] C.J. Briscoe, M.R. Stiles, D.S. Hage, System suitability in bioanalytical LC/MS/MS, J. Pharm. Biomed. Anal. 44 (2007) 484–491.

[30] I.-H. Baek, Dose proportionality and pharmacokinetics of dronedarone following intravenous and oral administration to rat, Xenobiotica 49 (2019) 734–739.

[31] B.P. Smith, F.R. Vandenhende, K.A. DeSante, et al., Confidence interval criteria for assessment of dose proportionality, Pharm. Res. 17 (2000) 1278–1283.

[32] J. Hummel, S. McKendrick, C. Brindley, et al., Exploratory assessment of dose proportionality: review of current approaches and proposal for a practical criterion, Pharm. Stat. 8 (2009) 38–49.

[33] M.L. Nan, Y.F. He, Y.W. Zhao, et al., Oral bioavailability study of rotundic acid in rats, China Pharm. 19 (2016) 1648–1650.

[34] B. Yang, H. Li, Q. Ruan, et al., Rapid profiling and pharmacokinetic studies of multiple potential bioactive triterpenoids in rat plasma using UPLC/Q-TOF-MS/MS after oral administration of Ilicis Rotundae Cortex extract, Fitoterapia 129 (2018) 210–219.

[35] B. Yang, H. Li, Q. Ruan, et al., Effects of gut microbiota and ingredient-ingredient interaction on the pharmacokinetic properties of rotundic acid and pedunculoside, Planta Med. 85 (2019) 729–737.

[36] B. Davies, T. Morris, Physiological parameters in laboratory animals and humans, Pharm. Res. 10 (1993) 1093–1095.

[37] K.W. Ward, L.M. Azzarano, W.E. Bondinell, et al., Preclinical pharmacokinetics and interspecies scaling of a novel vitronectin receptor antagonist, Drug Metab. Dispos. 27 (1999) 1232–1241.